CONFIDENTIAL

Copy 343
RM L54J28

NACA RM L54J28

NACA

RESEARCH MEMORANDUM

VIBRATORY-STRESS INVESTIGATION OF SIX- AND EIGHT-BLADE DUAL-ROTATING PROPELLERS OPERATING AT ZERO ADVANCE

By Atwood R. Heath, Jr. and Robert L. O'Neal

Langley Aeronautical Laboratory
Langley Field, Va.

NATIONAL ADVISORY COMMITTEE
FOR AERONAUTICS

WASHINGTON
February 4, 1955

CONFIDENTIAL

NATIONAL ADVISORY COMMITTEE FOR AERONAUTICS

RESEARCH MEMORANDUM

VIBRATORY-STRESS INVESTIGATION OF SIX- AND EIGHT-BLADE DUAL-ROTATING PROPELLERS OPERATING AT ZERO ADVANCE

By Atwood R. Heath, Jr. and Robert L. O'Neal

SUMMARY

An investigation of the vibratory stresses of a dual-rotating propeller of both six-blade and eight-blade configurations has been made on the NACA 6,000-horsepower propeller dynamometer at the Langley propeller static test stand. Particular attention was directed to the measurement of the vibratory stresses caused by the mutual blade interference of the front- and rear-propeller components. The investigation covered a range of blade angle from 4° to 36° and a range of rotational speed from 600 rpm to 2,200 rpm.

The results indicate that vibratory stresses caused by mutual excitation of the propeller blades were small in all bending modes of vibration, but large vibratory stresses were noted in the torsional mode of vibration.

The largest vibratory bending stresses occurred at twice the rotational frequency of the propeller in the fundamental propeller-blade bending mode during operation in a cross wind.

A certain amount of stall-flutter data is also presented.

INTRODUCTION

One type of vibration excitation present in dual-rotating propellers, that is not encountered in single-rotating installations, is caused by mutual interference of the propeller blades of the front and rear components. Previous investigations on propellers with thick airfoil sections, such as those reported in references 1 and 2, have shown that vibratory stresses caused by excitation of the blade passage were not serious. However, for the thin flexible propeller blades that are currently being considered, some concern has been expressed as to the magnitude of these stresses because of possible resonant conditions. The

aforementioned references showed that the stresses of mutual interference were resonant and would complicate any stress calculations because the amount of aerodynamic damping was uncertain. Therefore, an experimental investigation has been undertaken to ascertain the magnitude of the vibratory stresses caused by mutual interference.

An investigation of the vibratory-stress characteristics of an 8.75-foot-diameter dual-rotating propeller, having relatively thin airfoil sections and operating at zero advance, has been made at the Langley propeller static test stand. A dual-rotating propeller of both six- and eight-blade configurations and having NACA 8.75-(5)(05)-037 blades was used. The blade angles at the 0.75 radius were varied from 4° to 36° and the propeller rotational speeds ranged from 600 rpm to 2,200 rpm.

Although the main purpose of the investigation was to measure stresses of mutual interference, in the course of the tests some effects of cross wind on the propeller stresses were studied, and a partial stall-flutter boundary was determined.

SYMBOLS

b	width of blade chord, ft
b_r	blade semichord, ft
c_{l_d}	blade-section design lift coefficient
D	propeller diameter, ft
h	blade-section maximum thickness, ft
L	blade length (measured from dynamometer case), ft
m	blade-passage excitation factor
N	propeller rotational speed, rpm
n	propeller rotational speed, rps
R	radius to propeller tip, ft
r	radius to blade element, ft
V	blade-section velocity, ft/sec

x	fraction of propeller tip radius, r/R
β	blade-section angle, deg
ω_α	fundamental natural torsional frequency, radians/sec

Subscripts:

F	front component
R	rear component

APPARATUS

NACA 6,000-horsepower propeller dynamometer.- The two units of the NACA 6,000-horsepower propeller dynamometer were installed at the Langley propeller static test stand. Figure 1 is a three-quarter front view of the installation and shows the eight-blade propeller in operating position. The two components of the propeller were mounted between the dynamometer units and were operated independently of each other. Looking at the propeller from the rear, the front component rotated clockwise and the rear counterclockwise. Although the two units of the dynamometer operated independently of each other, equal rotational speeds were maintained to within 1/4 rpm. Rotational speeds were measured by means of shaft-tachometer readings that were matched with the known frequency of a tuning fork. A more complete description of the dynamometer is given in reference 3. No spinners were used for this investigation.

Propeller blades.- The propeller blades were NACA 8.75-(5)(05)-037 dual-rotating blades. The first number of the designation refers to the diameter of the propeller in feet. The remaining portion refers to the blade geometry at the 0.70-radius station: (5) indicates a design lift coefficient of 0.50, and (05) indicates a thickness ratio of 0.05. The final number, 037, indicates a solidity of 0.037 per blade. NACA 16-series airfoil sections were used for the blades which were made of solid aluminum alloy. Figure 2 shows the blade-form curves and developed plan form of the propeller blades. The blade chord is tapered from 9.226 inches at the 0.286 radius to 6.920 inches at the 0.950 radius, and the thickness ratio is diminished from 0.099 at the 0.286 radius to 0.037 at the 0.950 radius. The design advance ratio of the propeller was 4.2 at a forward Mach number of 0.8. A spacing of $13\frac{1}{8}$ inches between planes of the front- and rear-propeller components was maintained for the entire investigation.

Instrumentation.- Phenolic-bonded wire strain gages were used to measure the vibratory stresses. Strain gages arranged to measure flatwise bending stresses were distributed along the cambered surface of one blade of each of the front- and rear-propeller components. Strain gages for measuring torsional stress were located on the cambered surface of one blade of each propeller component at the 0.75-radius station for all tests of the six-blade configuration and part of the tests of the eight-blade configuration. Two other torsional gages were located on one other blade of each component at the 0.30-radius station and were operative for only part of the tests on each configuration. Shank bending was measured by gages located at 0°, 45°, and 90° related to the chord line at the 0.75-radius station on the same blade of the rear component as the flatwise bending gages. The strain-gage locations are shown on a developed plan form of the blade in figure 3. A limited number of amplifiers necessary for strain-gage operation were available so that only a part of the stress data could be obtained for any given test. Table I gives the number of strain gages and their locations for the various tests.

Filters that passed vibratory signals of only 90 cycles per second or higher were incorporated in the strain-gage circuits. The filters could be left in or left out of the circuits at will to allow signals of the total vibration, as well as the filtered vibration, to be recorded on a multichannel recording oscillograph.

TESTS

The investigation was made over a front blade-angle range of $\beta_{F(0.75R)} = 4^\circ$ to 36° with the rear blade angle at the 0.75 radius set 1° lower than the front blade angle. For the six-blade configuration at $\beta_{F(0.75R)} = 12^\circ$, tests were also made with the rear blade angle set 0° and 2° lower than the front blade angle.

The rotational speed of the propeller was increased by 100-rpm increments from around 600 rpm to a maximum of 2,200 rpm or to the safe-operating stress limits. Smaller increments of rotational speed were set when rapid increases in the vibratory stress for small increases in rotational speed were observed.

Table II presents a summary of the tests and shows the blade angles and the ranges of rotational speed in the strain-gage test groups for the two propeller configurations. Two tests not shown in the summary were made to determine the stress relation between torsional stresses measured at the 0.30 radius and those measured at the 0.75 radius. Most of the

tests were made with wind velocities in the test stand of 2.5 feet per second or less; however, the wind increased during several tests up to 3.3 to 5.0 feet per second.

The fundamental static natural frequencies of the propeller blades were measured with the blades installed on the dynamometer. The static natural frequencies for the higher modes of vibration were determined with the propeller hub bolted securely to a concrete block. The latter method was used because the equipment for precise excitation and measurement of the higher frequencies could not be used when the propeller was mounted on the dynamometer.

REDUCTION OF DATA

Total vibratory stress, bending or torsion, was considered to be the vibratory stress without regard to the frequencies present. Since the total vibratory stress varied erratically with time for each test point, the maximum recorded stresses will be presented.

Each stress record was analyzed to determine the magnitude of the component of vibratory stress at blade-passage frequency. Most of the data could be analyzed by the envelope method of reference 4. For many tests, the stress at blade-passage frequency combined with stress at an adjacent order of propeller vibration to give a beating waveform. However, for some tests no waveform analysis was necessary because the filters in the strain-gage circuits passed a signal only at blade-passage frequency to the recording oscillograph. Several stress records required the use of the method of superposition given in reference 4 to determine blade-passage stresses.

For comparison with the torsional stresses of the six-blade configuration which were measured at $x = 0.75$, the torsional stresses of the eight-blade configuration measured at $x = 0.30$ have been adjusted to values of stress that would have been measured at $x = 0.75$ had the strain gages been operative. The adjustment was made by using factors obtained from the two tests in which the stresses at the two stations were read simultaneously.

The torsional vibratory stresses measured during stall flutter were also analyzed by the previously noted methods to obtain only that component of stress at the fundamental torsional natural frequency of the blade. Such a procedure was necessary because stresses at blade-passage frequency of the same magnitude as the flutter stresses were observed at one blade angle.

RESULTS AND DISCUSSION

Vibratory Stress at Propeller-Blade-Passage Frequency

Propeller-blade frequency spectrum.- The orders of vibration at the blade-passage frequency for this investigation were six times the propeller frequency 6xP for the six-blade configuration, and 8xP for the eight-blade configuration. The vibratory stresses at blade-passage frequency occurred only in several distinct rotational speed ranges of the propeller and were not in evidence over the entire operating range. The different modes of vibration were determined from the type of strain gage (bending or torsion), from the stress distributions over the blade, and from the phase relationships of the stresses over the blade. In each mode of vibration, the stress variation with the rotational speed of the propeller indicated a resonant condition.

Figure 4 shows the approximate measured resonant frequencies, the measured static natural frequencies of the propeller blade, and the propeller orders of excitation. The static natural frequencies were slightly different for each blade; therefore, average values are given. The curves have been drawn to tie together related points and will only approximate the variation of the natural frequencies with propeller rotational speed. In the case of the bending modes, the rotational natural frequencies would be expected to vary with blade angle, but the frequencies could not be determined with sufficient accuracy to show any definite variation; therefore, approximate values are given. The only modes of vibration at blade-passage frequency detectable in the operating range were fundamental edgewise bending, second and third flatwise bending, and fundamental torsion.

Vibratory torsional stresses.- The largest vibratory stresses caused by mutual interference of the propeller blades were found to be in the fundamental torsional mode. Figures 5 and 6 show the variation of the torsional stress with propeller rotational speed for the six- and eight-blade configurations, respectively. Resonance is noted in the vicinity of 1,700 rpm for the six-blade configuration, and 1,300 rpm for the eight-blade configuration. Because of the slight differences in the torsional natural frequencies of the different blades, the stress curves have been drawn to show resonance at the static natural frequency of the blade for which the data were obtained.

In order to show the effect of blade angle on the stress and to compare the stresses of the front and rear components, the stresses were read at the same approach to resonance $\frac{2\pi nm}{\omega_\alpha} = 0.936$ and are presented

in figure 7 as a function of the front-component blade angle. A definite increase of stress with blade angle is noted for all blades. For the data of figure 7, a constant difference in blade angle of 1° between the front and rear components was maintained over the range of blade angle. This constant difference in blade angle does not represent a constant difference in power absorption between the two components. In order to show that the increase of stress with blade angle was caused by the blade loadings and not by the difference in blade loadings, the rear blade angle was set 0° and 2° lower than the front blade angle (12°), to vary the difference in power absorption of the two components. The stresses of each component remained constant for the three tests which represented ratios of rear-component power to front-component power of 1.010, 0.738, and 0.555. Therefore, the increase of stress with blade-angle increase may be attributed to an increase in the loading on the propeller blades. The increase of stress with increased loading is also noticed in a comparison of the six- and eight-blade configuration stresses of figure 7. For any given blade angle over 4°, the stresses of the six-blade configuration which were measured near 1,700 rpm are higher than the stresses of the eight-blade configuration which were measured near 1,300 rpm.

Figure 7 also shows that the rear-component blade stresses were higher than the front-component blade stresses. Such an effect seems possible when it is considered that the rear component operated wholly in the slipstream of the front component, while the front was subjected only to the relatively smaller induced effects ahead of the rear component.

Although the maximum measured torsional stresses are below ±6,000 pounds per square inch, it appears (fig. 5(b)) that larger stresses would have been encountered for some blade-angle tests if the propeller rotational speed had been increased. In view of the possibility of large stresses in torsion for ground operation, care should be taken in the design of a constant-speed variable blade-angle propeller installation to insure that the torsional natural frequency of the blades does not coincide with the blade-passage frequency.

Vibratory bending stresses.- The largest vibratory stresses measured in any bending mode were in the second flatwise bending mode. Figure 8(a) shows typical radial vibratory-stress distributions for the front- and rear-component blades in this mode. The maximum measured stress occurred at the 0.75 station where the stress on the rear-component blade was about twice that on the front blade.

Figure 8(b) shows radial vibratory flatwise bending-stress distributions similar in shape to those of figure 8(a), but resulting from an edgewise bending mode. The shank strain-gage stress readings were very small (less than ±300 pounds per square inch), but the stresses indicated that the vibration was principally edgewise with respect to the

0.75 radius; this condition would indicate fundamental edgewise bending. Although the vibration mode was edgewise, the coupling effects due to blade twist caused a flatwise stress distribution over the blade similar to second bending. An experimental investigation of the coupling effects of blade twist has been reported in reference 5 in which a flatwise stress distribution similar to third bending was obtained in the edgewise mode of vibration.

For the two modes of vibration of figure 8 the maximum measured stress at 0.75 radius is presented as a function of blade angle in figure 9. The stresses are rather erratic, no doubt due to the fact that the resonant stress was not recorded in each instance; but for each mode of vibration, the stress trend increases with increasing blade angle. At the lower blade angles, there is little difference between stresses on the front- and rear-component blades, but at the higher blade angles, the rear-component blade stresses are in most instances higher than the front as was noted for the torsional stresses. The stress levels, however, are low in magnitude and may be considered unimportant.

The propeller rotational speed for third flatwise bending vibration was reached for only a few of the tests, and the stresses were very small in all cases (less than ± 400 pounds per square inch).

Total Vibratory Stress

The variations of total vibratory stress with propeller rotational speed for flatwise-bending and torsional vibration in the six-blade configuration at $\beta_{F(0.75R)} = 8^{\circ}$ and $\beta_{R(0.75R)} = 7^{\circ}$ are shown in figure 10. In general, the shapes of the distribution are typical of all the tests; however, for the higher blade-angle tests, stress levels as much as 100 percent higher than those shown in figure 10 were measured. The only increase in bending stresses over the general level occurred at 900 rpm and is most noticeable in figures 10(a), (b), (c), (e), (g), and (i) for test group I. The stress at the aforementioned rotational speed was resonant and was due to the coincidence of the fundamental natural bending frequency of the propeller blade with an excitation at twice the propeller rotational frequency 2xP. These 2xP stresses were attributed to a cross wind in the test stand of about 3.3 feet per second. Although the primary effect of a cross wind on propeller operation is to cause a 1xP vibration, it has been shown in the analysis of reference 6 for a helicopter in forward flight, which closely simulates the present cross-wind-propeller condition, that the 1xP excitation is not a pure sine wave and that a 2xP component exists. The 2xP excitation is small with respect to the 1xP excitation, but large 2xP stresses can result from amplification of the stress at resonance. Figures 10(a) and (b) show that, for a test made at a different time (test group II) during which no wind

was blowing, no large increase in stress occurred near 900 rpm. Reference 6 shows that the 2xP excitation varies as the square of the cross-wind velocity. Therefore, the operating limit of the vibratory stress (±6,000 pounds per square inch) set for this investigation would have been reached with a cross wind of about 4.2 feet per second if the maximum stress of figure 10(b), (±3,940 pounds per square inch obtained during a cross wind of about 3.3 feet per second) were to be extrapolated. Thus it appears that this propeller may encounter large 2xP stresses during normal ground operation.

The only other large increase of vibratory stress over the general stress level was in the torsional mode of vibration and is shown in figures 10(k) and 10(l) around 1,700 rpm. Analysis indicated that the stress increases were due to mutual interferences on the front and rear components of the propeller which have been more fully discussed in the preceding sections.

Stall-Flutter Boundaries

Partial stall-flutter boundaries were obtained for the front and rear components of both the six- and eight-blade configurations. Figure 11 shows these boundaries which were based on a torsional stress of ±2,000 pounds per square inch at the torsional natural frequency of the blade. The stress value of ±2,000 pounds per square inch was chosen for comparison of the flutter characteristics of the propellers because it was the largest stress measured for some tests. A stress value had to be chosen as a flutter criterion because the flutter was intermittent in nature. No consistent differences were noted between the flutter characteristics of the six- and eight-blade configurations. No significance can be attached to this occurrence because the repeatability of flutter points was frequently good to only 10 percent of the flutter-speed coefficient. The rear-component blades had a flutter-speed coefficient $\left(\frac{V}{b_r \omega_\alpha}\right)_{0.8L}$ that was about 0.20 less than the front blades. It could not be determined from the present investigation whether the lower flutter-speed coefficient would be realized if sustained flutter were to be encountered. However, the onset of stall flutter occurs on the rear-component propeller at a lower rotational speed than the front component, and it is thought that this effect may be partially caused by excitation from the wake of the front component, even though the frequency of the mutual excitation was not at the fundamental torsional natural frequency of the blade.

For comparison of the flutter characteristics of the front-component blades with a single-rotating propeller, stall-flutter data for the

NACA 10-(5)(066)-03 three-blade propeller reported in reference 7 have been included in figure 11. A slightly different blade reference station for the flutter-speed coefficient was used in reference 7 so the data have been adjusted to the same blade reference station as that used for the present tests. The NACA 10-(5)(066)-03 blades were chosen for comparison because they had the same design lift coefficient at the 0.70 station as the dual-rotating propellers and had a difference in thickness ratio of only 0.016.

The minimum flutter coefficient of the single-rotating propeller is 1.06 while that for the front component of the dual-rotating propeller is 0.99. It should be noted that the flutter curve for the single-rotating propeller marks the boundary of sustained flutter while the curve for the dual-rotating propeller marks a certain stress value in intermittent flutter. If sustained flutter had been reached on the dual-rotating propeller, better agreement with the minimum flutter coefficient of the single-rotating propeller might have been obtained.

Although only approximate agreement in minimum flutter coefficient of the two propellers was obtained, it is believed that the comparison presents sufficient evidence that the flutter coefficient of the front component of the dual-rotating propeller was not significantly different from that of a similar unit operating by itself.

CONCLUSIONS

From the present investigation of the vibratory-stress characteristics of a dual-rotating propeller having thin airfoil sections and operating at zero advance, the following conclusions can be drawn:

1. Large vibratory stresses in the torsional mode of vibration can occur if the frequency of the mutual excitation of the propeller blades coincides with the fundamental torsional natural frequency of the blade.

2. Vibratory stresses caused by mutual excitation of the propeller blades were very small in all bending modes of vibration.

3. Large vibratory bending stresses at twice the rotational frequency of the propeller may be encountered during operation in a cross wind.

Langley Aeronautical Laboratory,
National Advisory Committee for Aeronautics,
Langley Field, Va., October 13, 1954.

REFERENCES

1. Krausnick, Walter S., and Conner, R. F.: Propeller Vibration Investigation of Hamilton Standard Four-Blade Dual-Rotation Propeller – Blade Designs 3155-6 & 3156-6; Hub Designs 5978-G & 52084-A – Run on Pratt & Whitney R-1830-13 Engine on P-36 Airplane. ACTR No. 4572, Materiel Div., Army Air Corps, Oct. 31, 1940.

2. Miller, Mason F.: Wind-Tunnel Vibration Tests of Dual-Rotating Propellers. NACA WR L-405, 1943. (Formerly NACA ARR 3I11.)

3. Wood, John H., and Swihart, John M.: The Effect of Blade-Section Camber on the Static Characteristics of Three NACA Propellers. NACA RM L51L28, 1952.

4. Manley, R. G.: Waveform Analysis. John Wiley & Sons, Inc. (New York), 1945.

5. Shannon, J. F., and Forshaw, J. R.: Propeller Blade Vibration: Nature and Severity of Vibration at Edgewise Resonance as Influenced by Coupling Effects Due to Blade Twist. R. & M. No. 2561, British A.R.C., May 1941.

6. Glauert, H.: Airplane Propellers. Helicopter Airscrews. Vol. IV of Aerodynamic Theory, div. L, ch. X, W. F. Durand, ed., Julius Springer (Berlin), 1935, pp. 318-320.

7. Allis, Arthur E., and Swihart, John M.: The Effect of Blade-Section Camber on the Stall-Flutter Characteristics of Three NACA Propellers at Zero Advance. NACA RM L53B17, 1953.

TABLE I

STRAIN-GAGE LOCATIONS FOR VARIOUS TESTS

Type of gage	Bending and torsional gage locations, x					
	Test groups I and IV		Test groups II and V		Test group III	
	Front	Rear	Front	Rear	Front	Rear
Bending	0.30	0.30	0.30	0.30	0.30	0.30
Bending	.45	----	----	.45	----	----
Bending	.60	----	----	.60	----	----
Bending	.75	----	----	.75	----	0.75
Bending	.90	----	----	.90	----	----
Torsion	.30	.30	.75	.75	.75	.75
Torsion	[a].75	[a].75	----	----	----	----
	Shank gage angular location, deg					
	Test groups I and IV		Test groups II and V		Test group III	
	Front	Rear	Front	Rear	Front	Rear
Shank	----	----	----	----	----	[b]0
Shank	----	----	----	----	----	[b]45
Shank	----	----	----	----	----	[b]90

[a] Not present for test group IV

[b] Related to 0.75 radius chord line

TABLE II

SUMMARY OF TESTS

$\beta_{(0.75R)}$, deg		Ranges of propeller speed, rpm				
		Six-blade configuration			Eight-blade configuration	
Front	Rear	Test Group I	Test Group II	Test Group III	Test Group IV	Test Group V
4	3	600 to 2,200	----------	----------	600 to 2,000	600 to 2,100
8	7	600 to 2,200	600 to 2,200	----------	600 to 1,500	----------
12	10	600 to 1,650	600 to 1,650	----------	----------	----------
12	11	600 to 1,650	----------	----------	600 to 2,000	----------
12	12	600 to 1,650	600 to 1,650	600 to 1,650	----------	----------
16	15	600 to 1,625	600 to 1,600	----------	600 to 1,175	600 to 1,200
20	19	600 to 1,423	----------	----------	500 to 1,450	----------
28	27	600 to 1,000	----------	600 to 975	600 to 1,175	600 to 1,000
36	35	550 to 835	----------	----------	500 to 925	----------

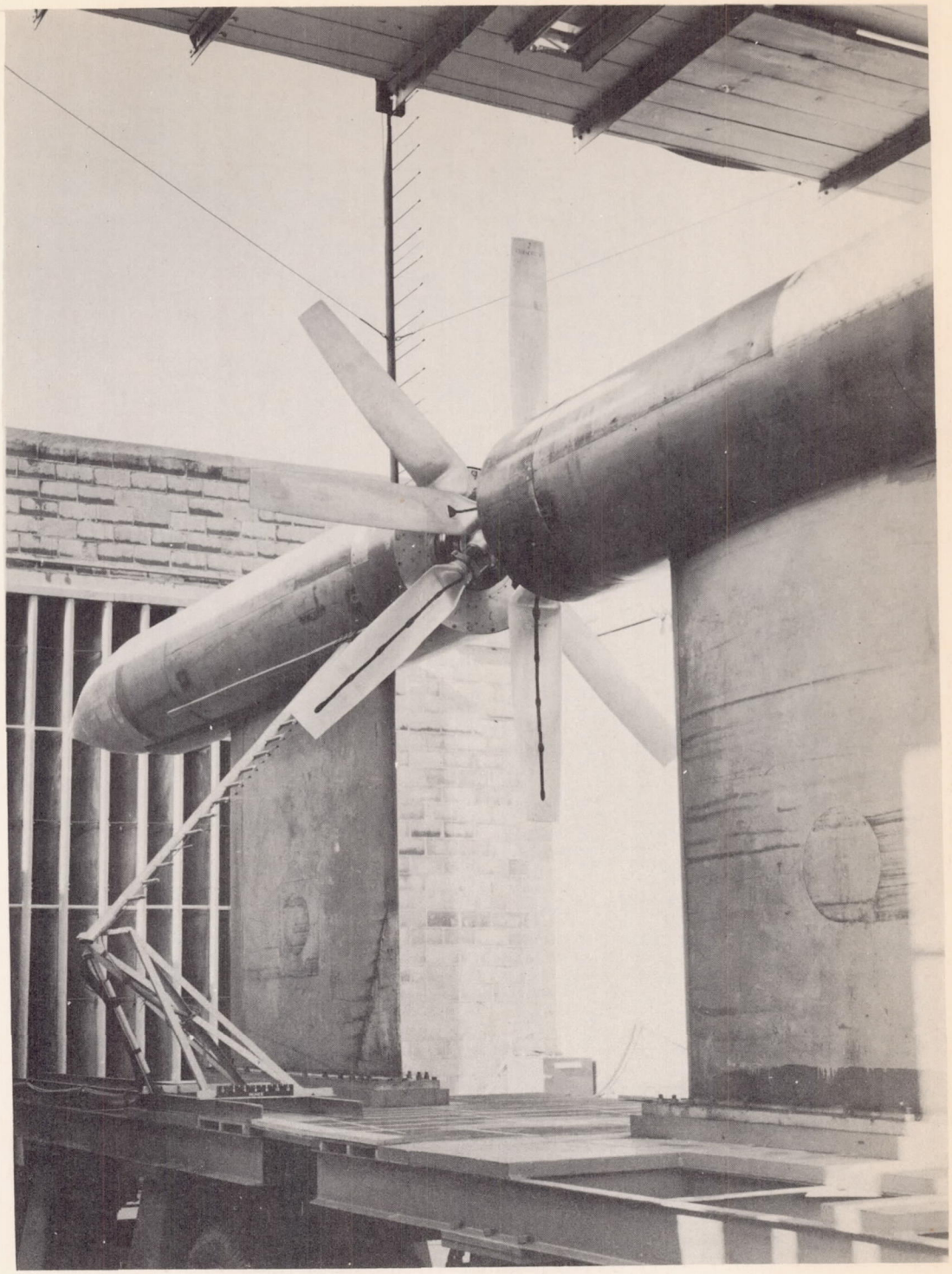

L-78831.1

Figure 1.- Three-quarter front view of the 8-blade configuration of NACA 8.75-(5)(05)-037 dual-rotating propeller installed on NACA 6,000-horsepower propeller dynamometer in Langley propeller static test stand.

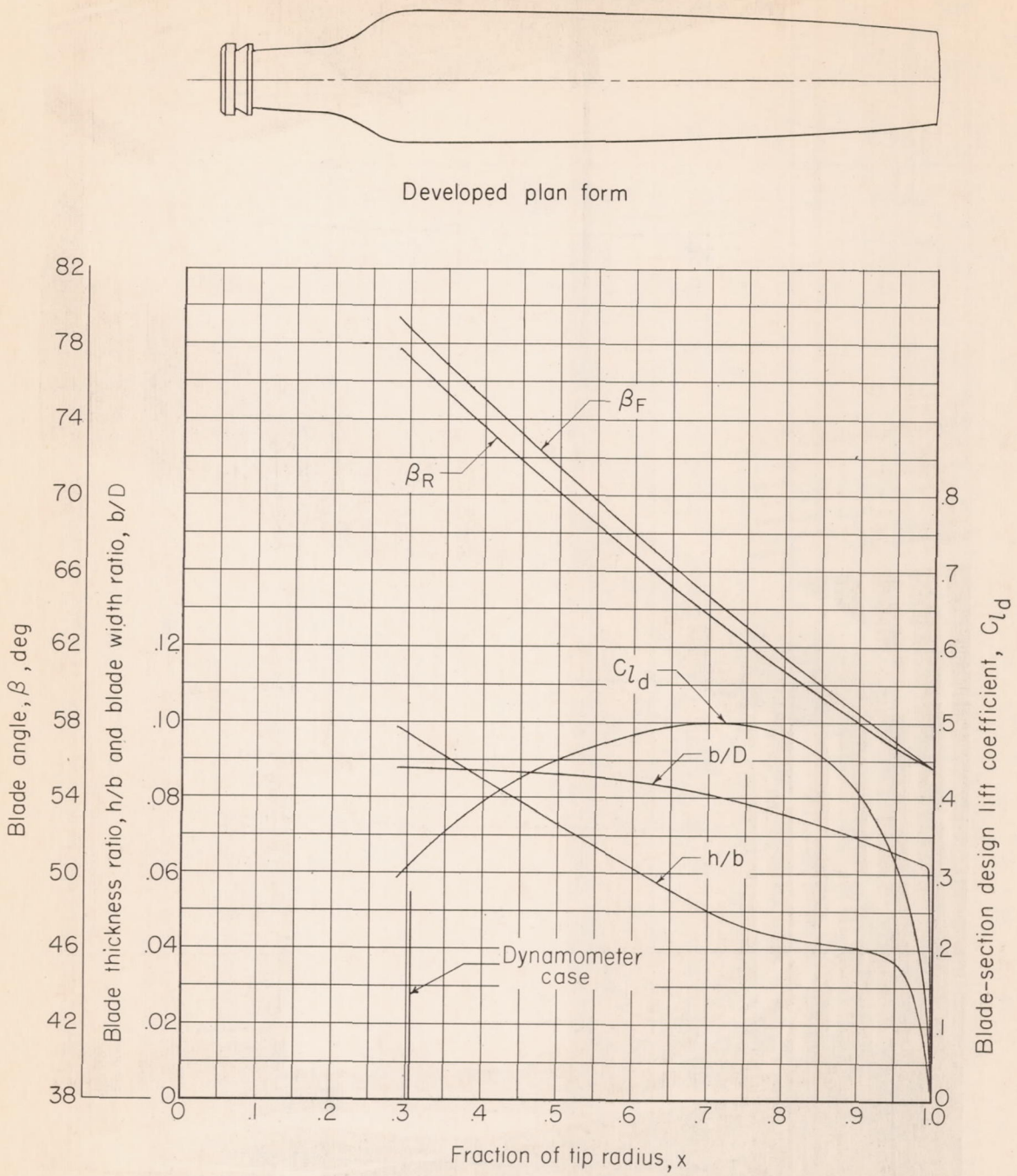

Figure 2.- Blade-form curves and developed plan form for NACA 8.75-(5)(05)-037 dual-rotating propeller.

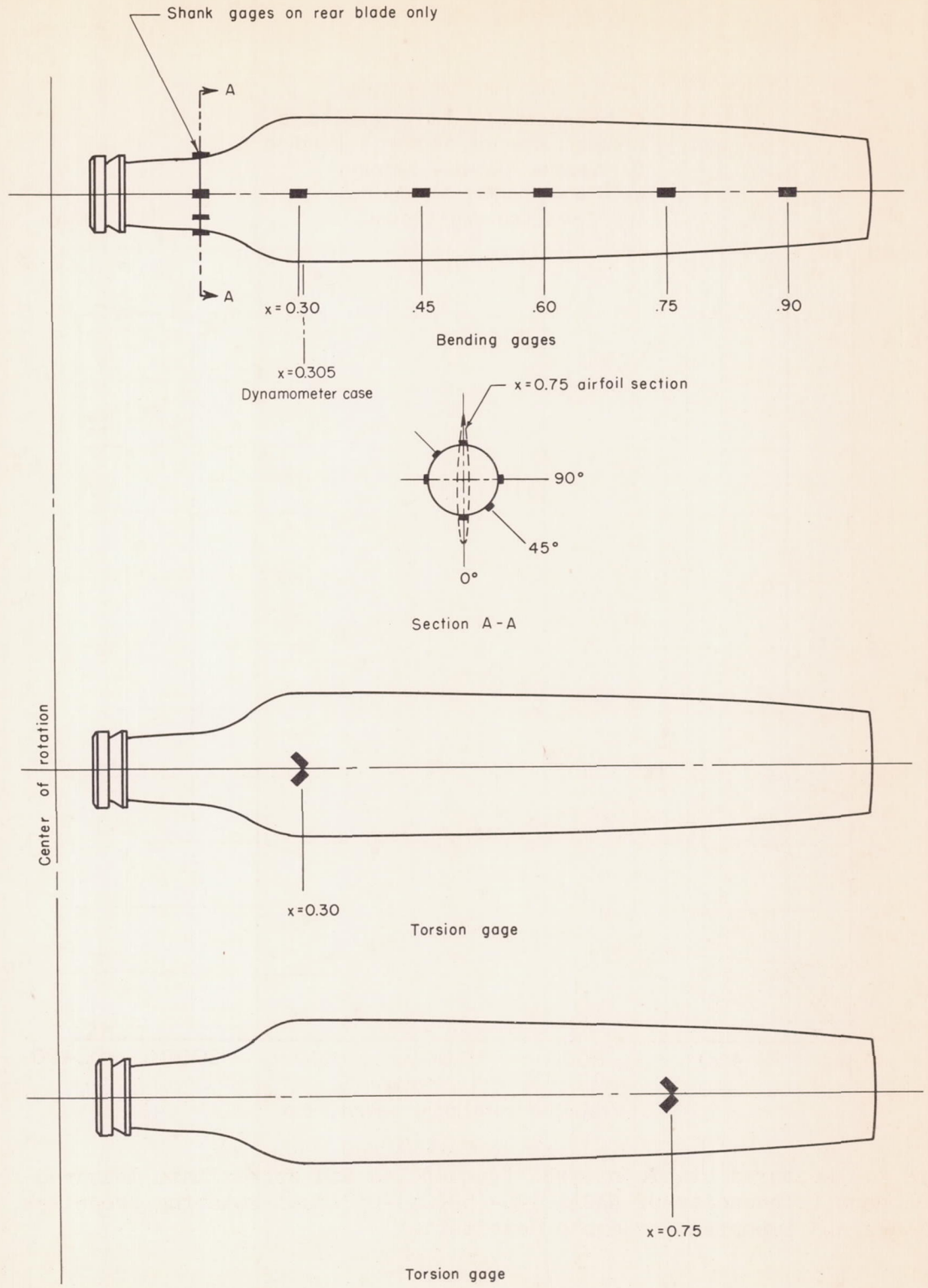

Figure 3.- Developed plan form of NACA 8.75-(5)(05)-037 dual-rotating propeller showing strain-gage locations.

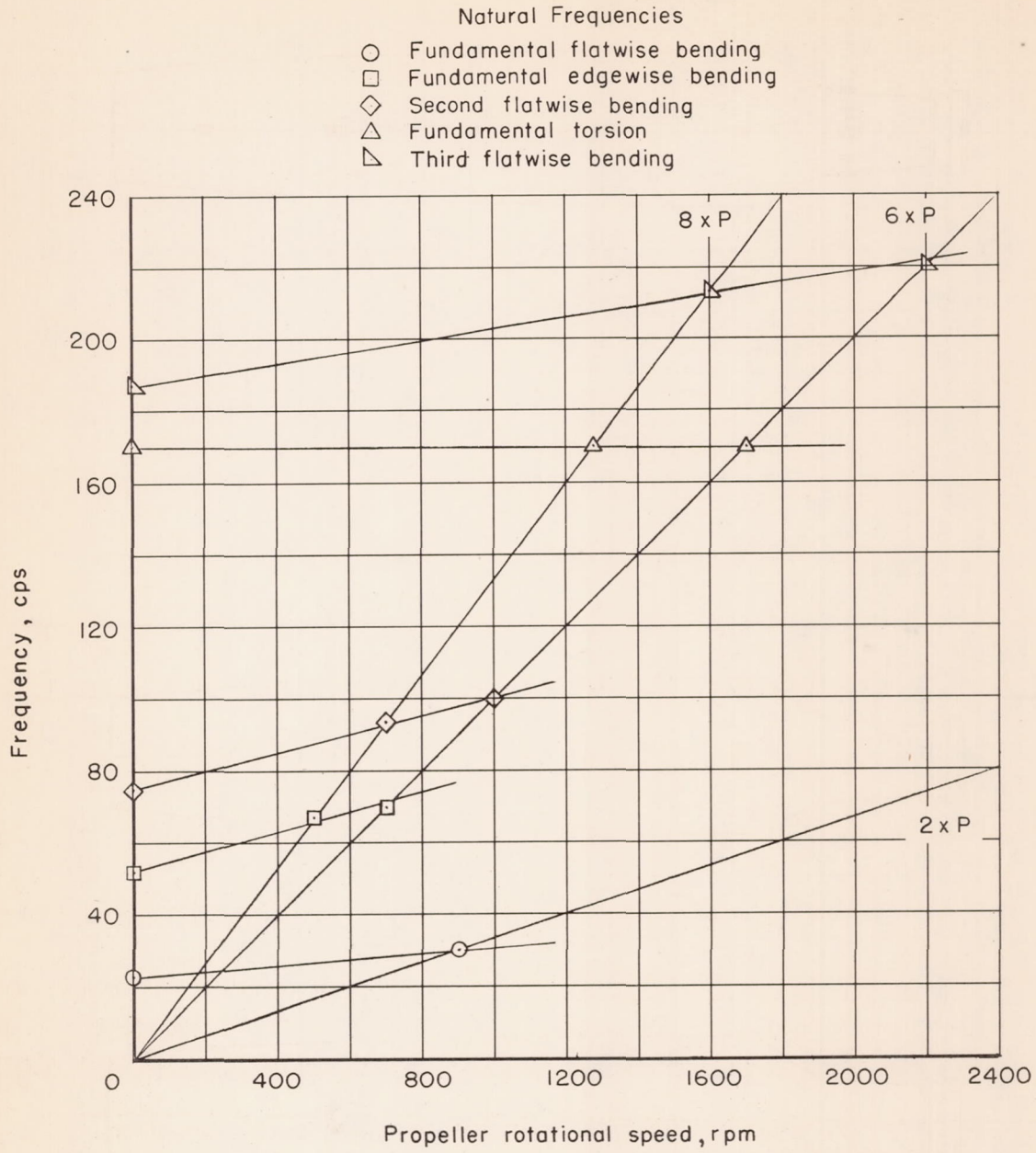

Figure 4.- Measured static natural frequencies and approximate measured resonant frequencies of NACA 8.75-(5)(05)-037 dual-rotating propeller blades and important orders of excitation.

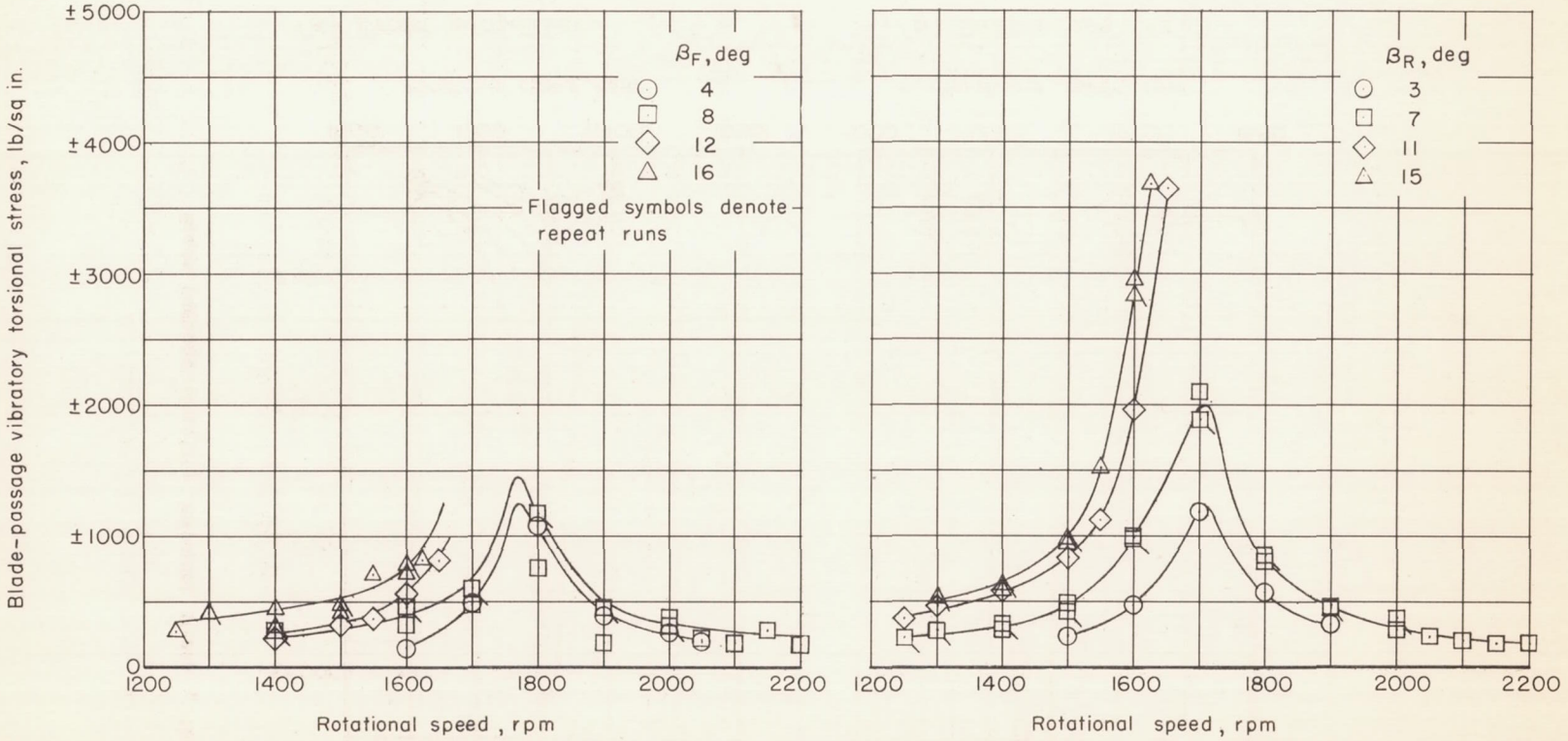

(a) Front propeller.

(b) Rear propeller.

Figure 5.- Variation of blade-passage vibratory torsional stress with rotational speed for front and rear propellers. Six-blade configuration at x = 0.75.

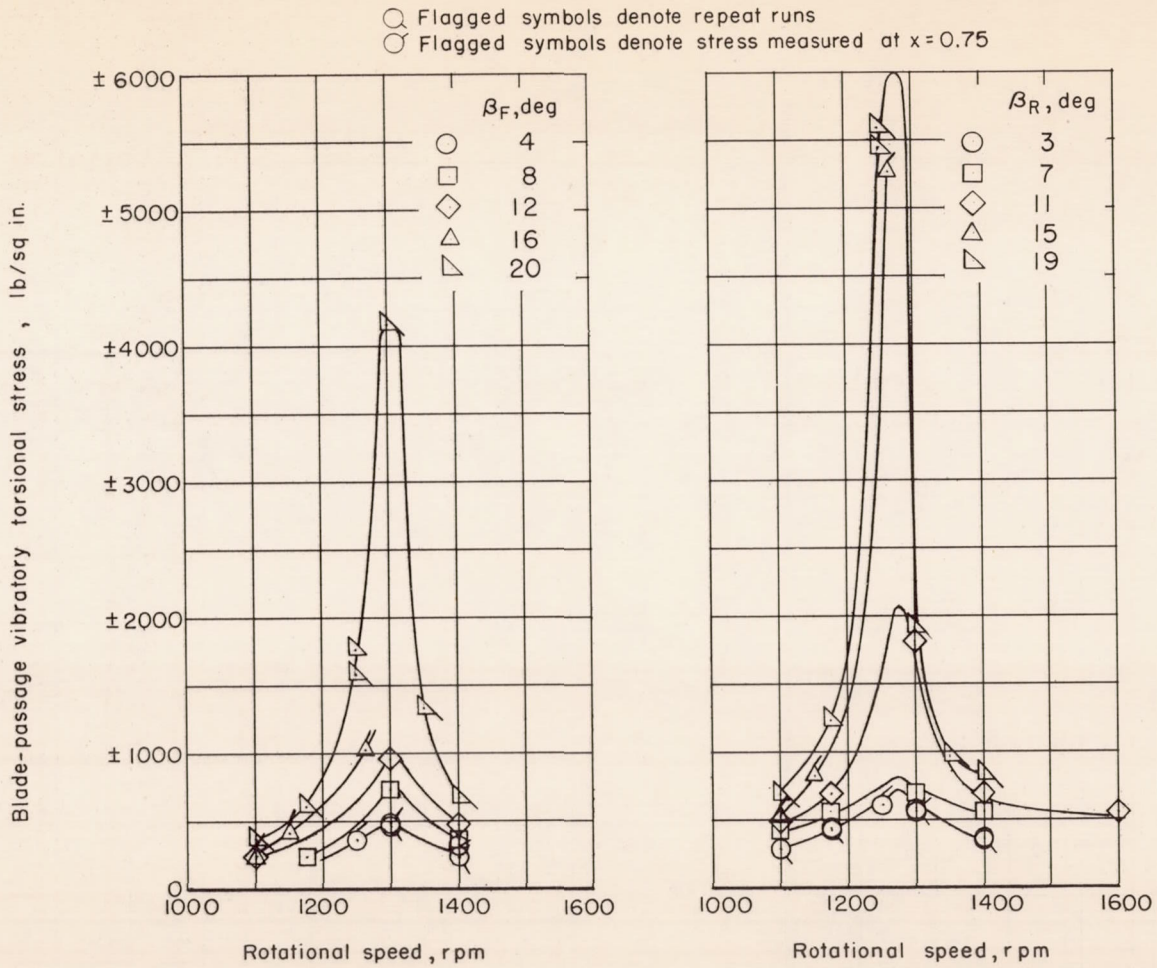

(a) Front propeller.

(b) Rear propeller.

Figure 6.- Variation of blade-passage vibratory torsional stress with rotational speed for front and rear propellers. Eight-blade configuration at $x = 0.75$. Stress measured at $x = 0.30$ but converted to stress at $x = 0.75$ by proportionality factor.

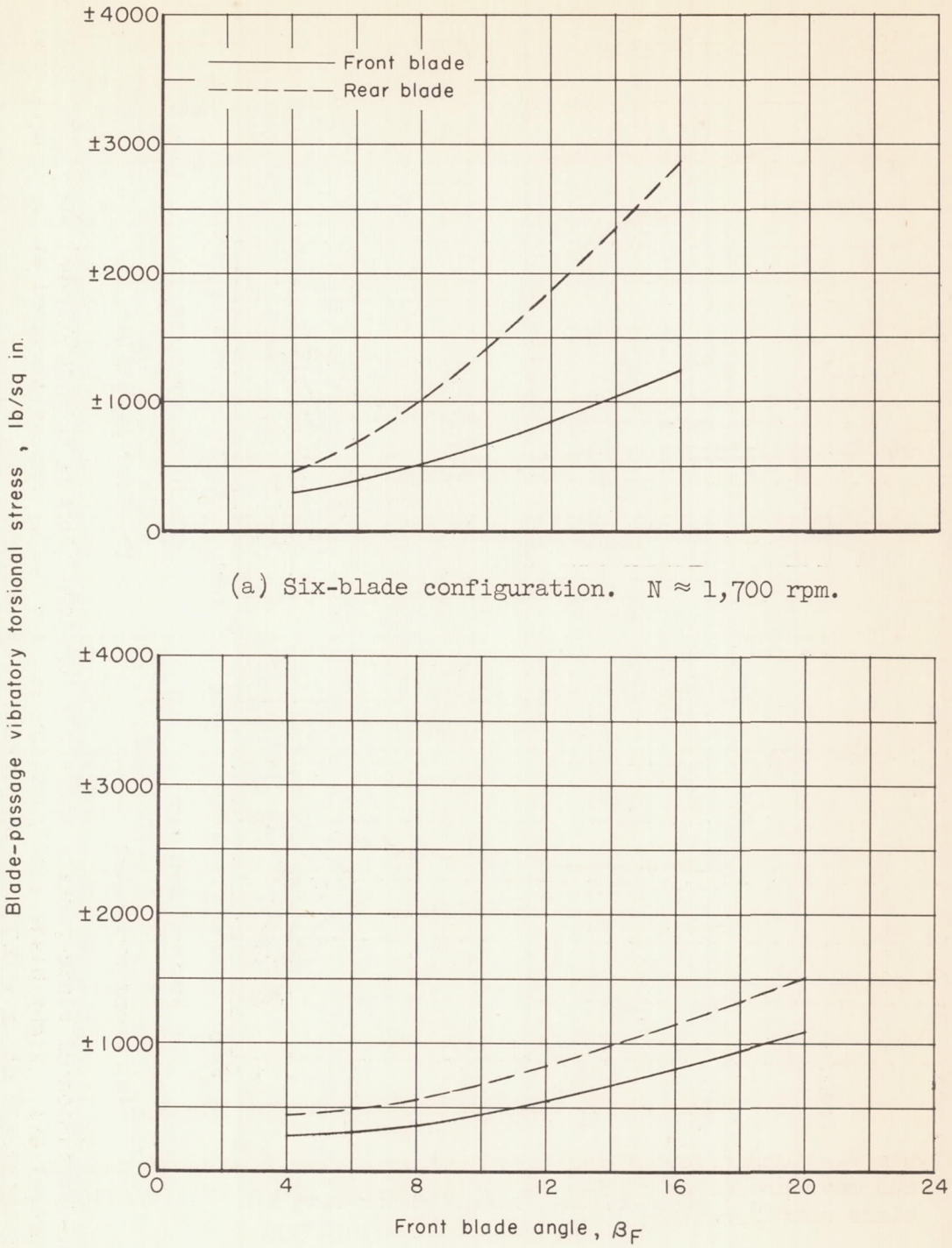

(a) Six-blade configuration. $N \approx 1{,}700$ rpm.

(b) Eight-blade configuration. $N \approx 1{,}300$ rpm.

Figure 7.- Variation of blade-passage vibratory torsional stress with front blade angle. $\frac{2\pi nm}{\omega_\alpha} = 0.936$.

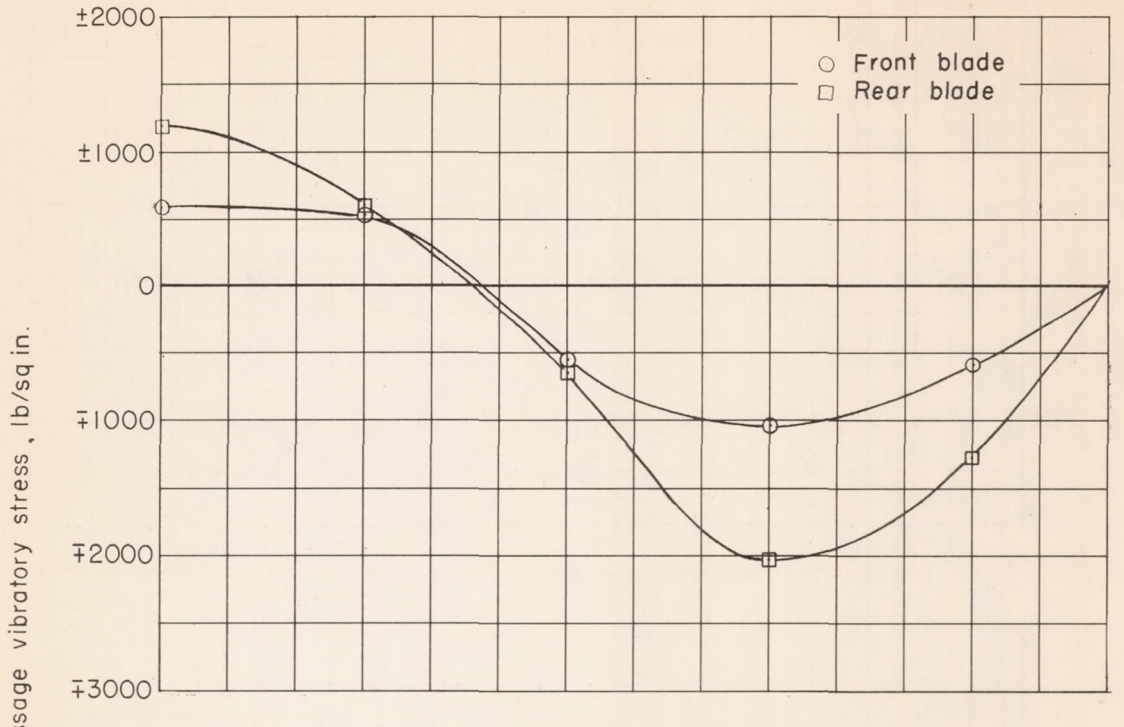

(a) Second flatwise bending mode. 1,000 rpm.

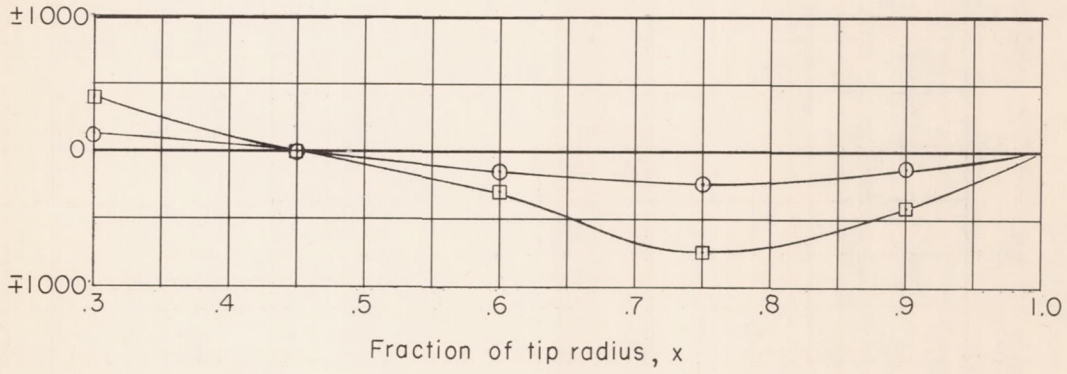

(b) Fundamental edgewise bending mode. 700 rpm.

Figure 8.- Comparison of radial vibratory stress distributions for front and rear propeller blades in two different modes of vibration. Six-blade configuration; $\beta_{F(0.75R)} = 16^{\circ}$; $\beta_{R(0.75R)} = 15^{\circ}$.

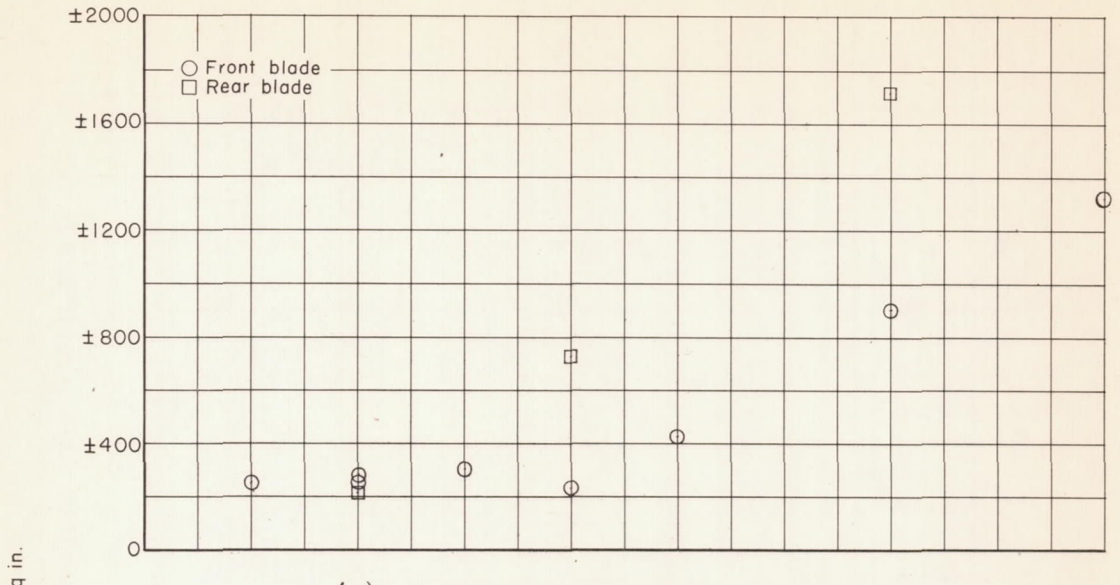

(a) Fundamental edgewise bending mode.

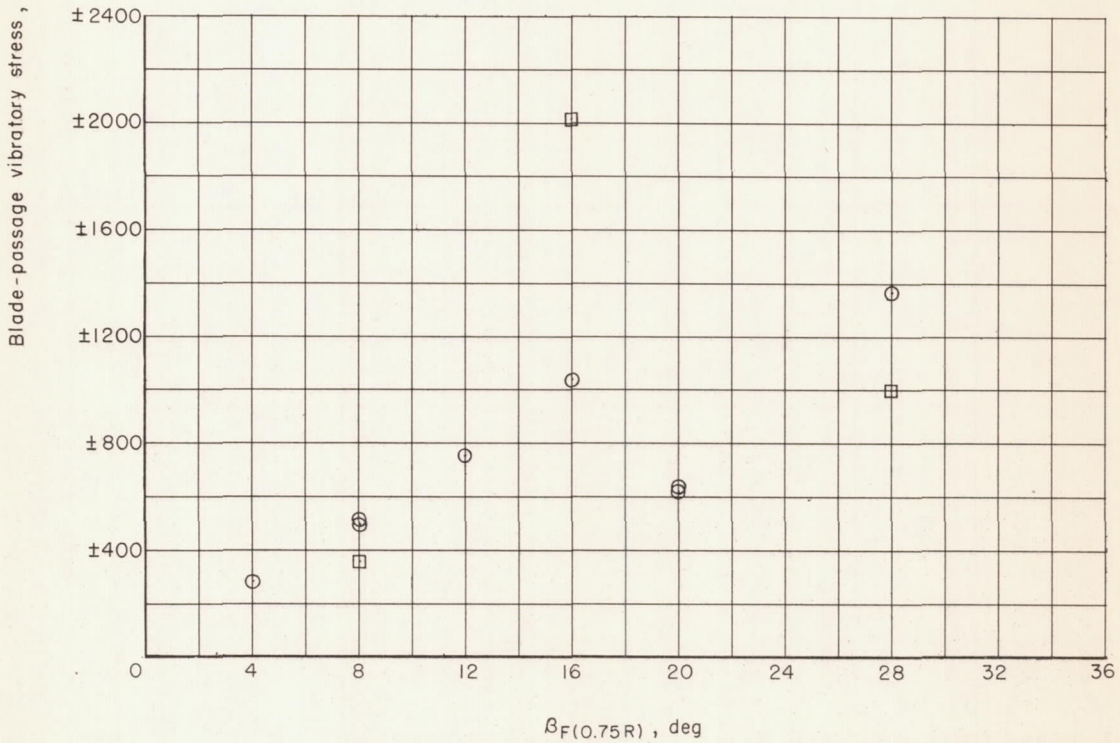

(b) Second flatwise bending mode.

Figure 9.- Variation of maximum measured vibratory stress near resonance in two different bending modes with propeller-blade angle for six-blade configuration. x = 0.75.

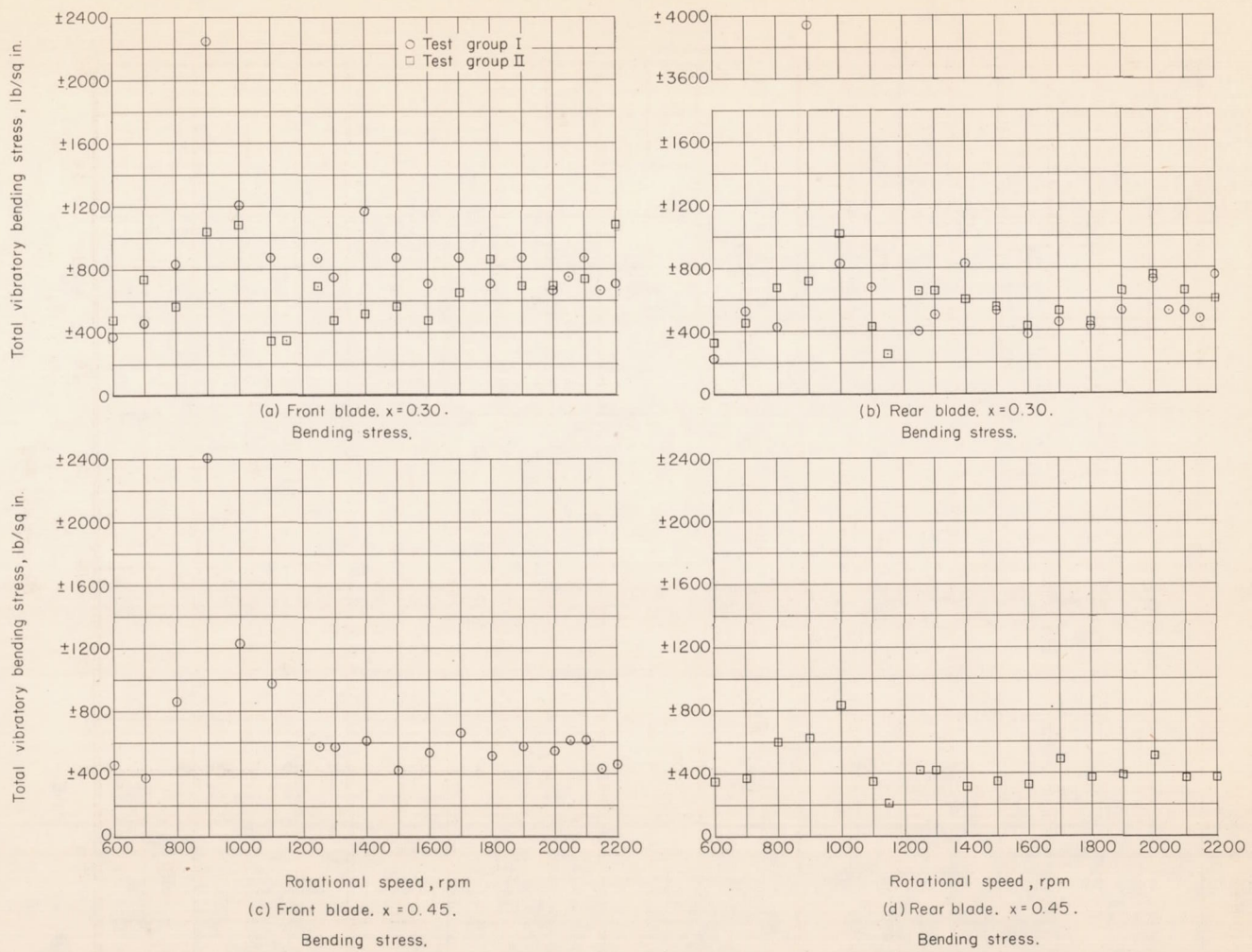

Figure 10.- Variation of total vibratory stress with propeller rotational speed at $\beta_{F(0.75R)} = 8^{\circ}$ and $\beta_{R(0.75R)} = 7^{\circ}$. Six-blade configuration; test group I.

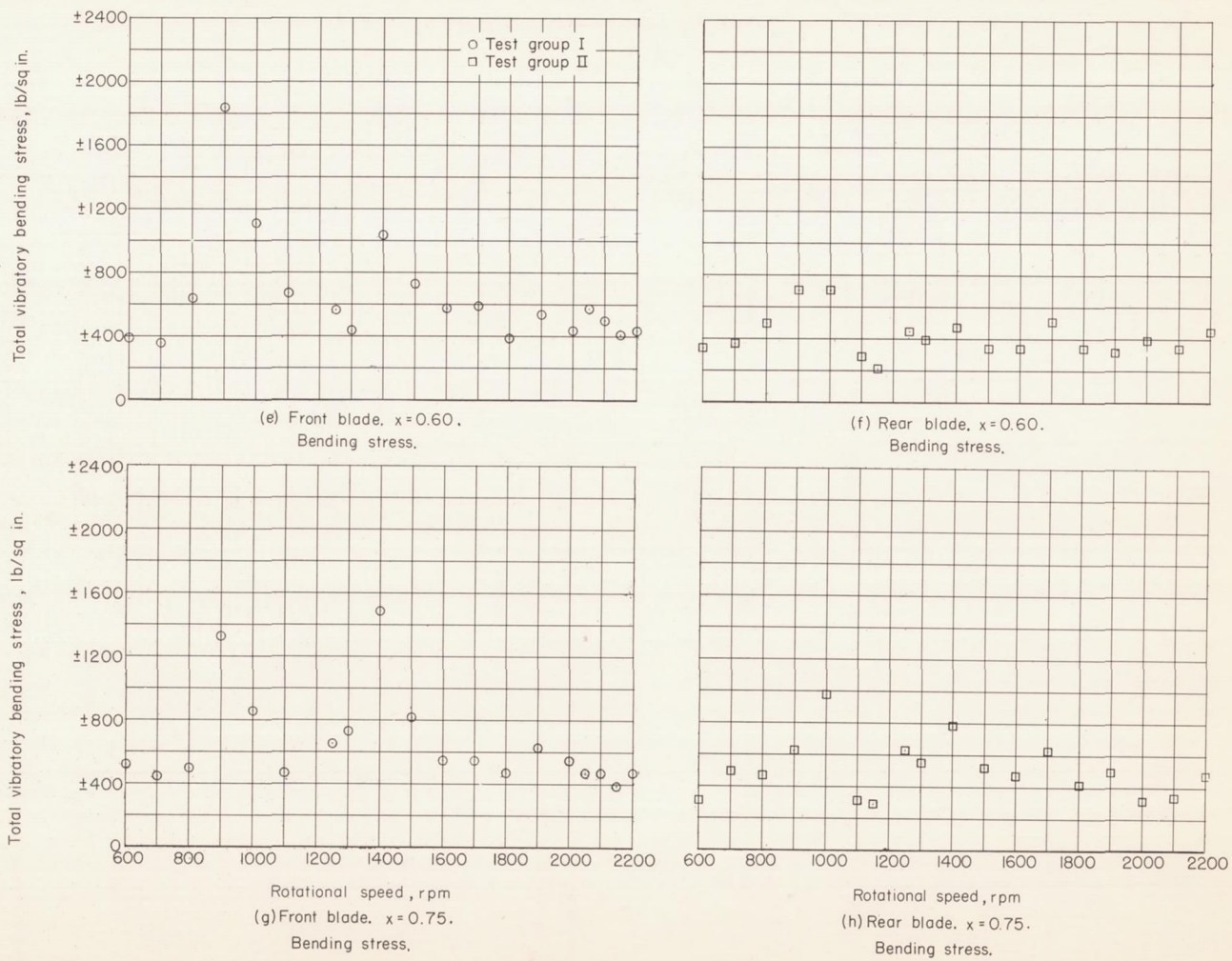

Figure 10.- Continued.

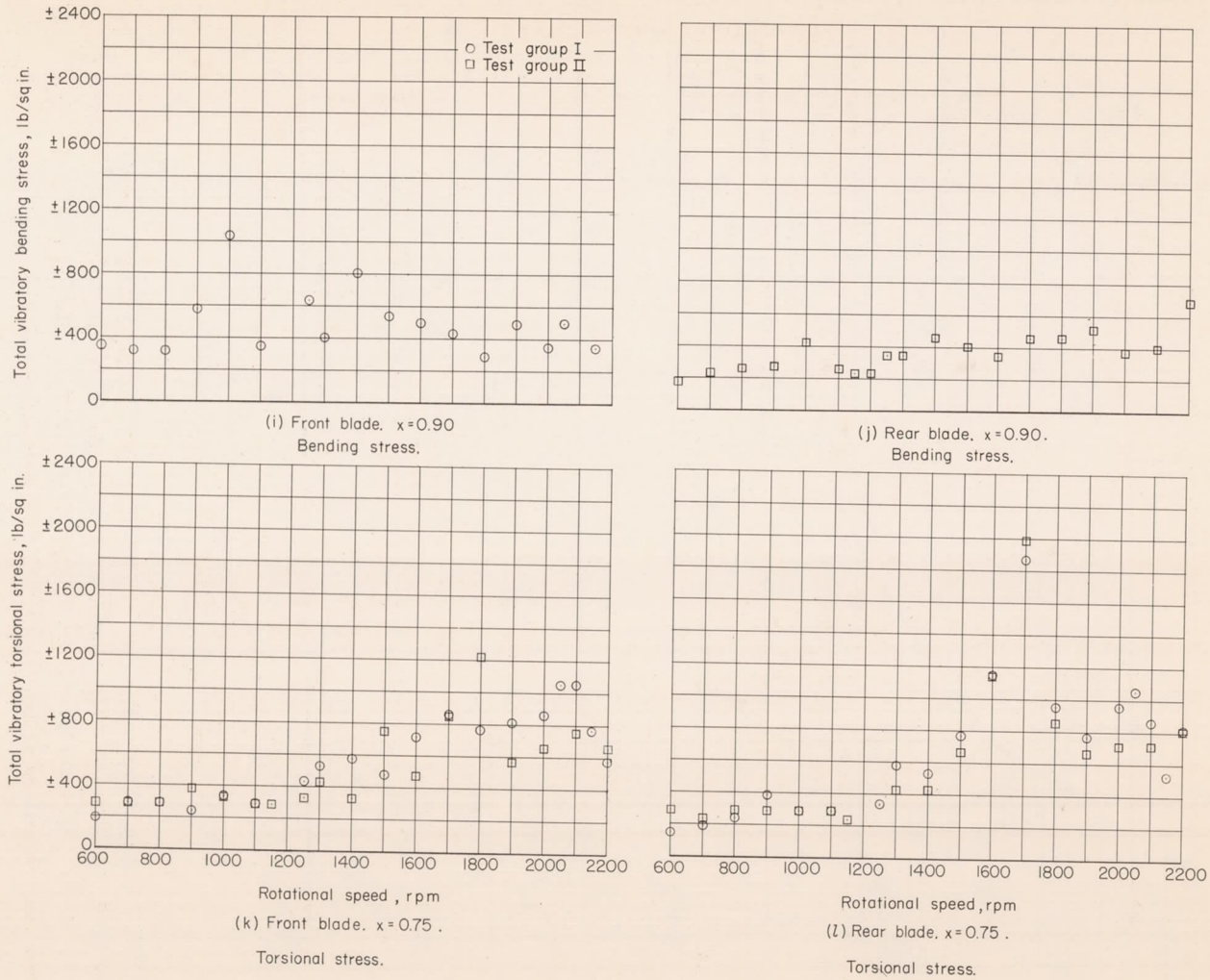

Figure 10.- Concluded.

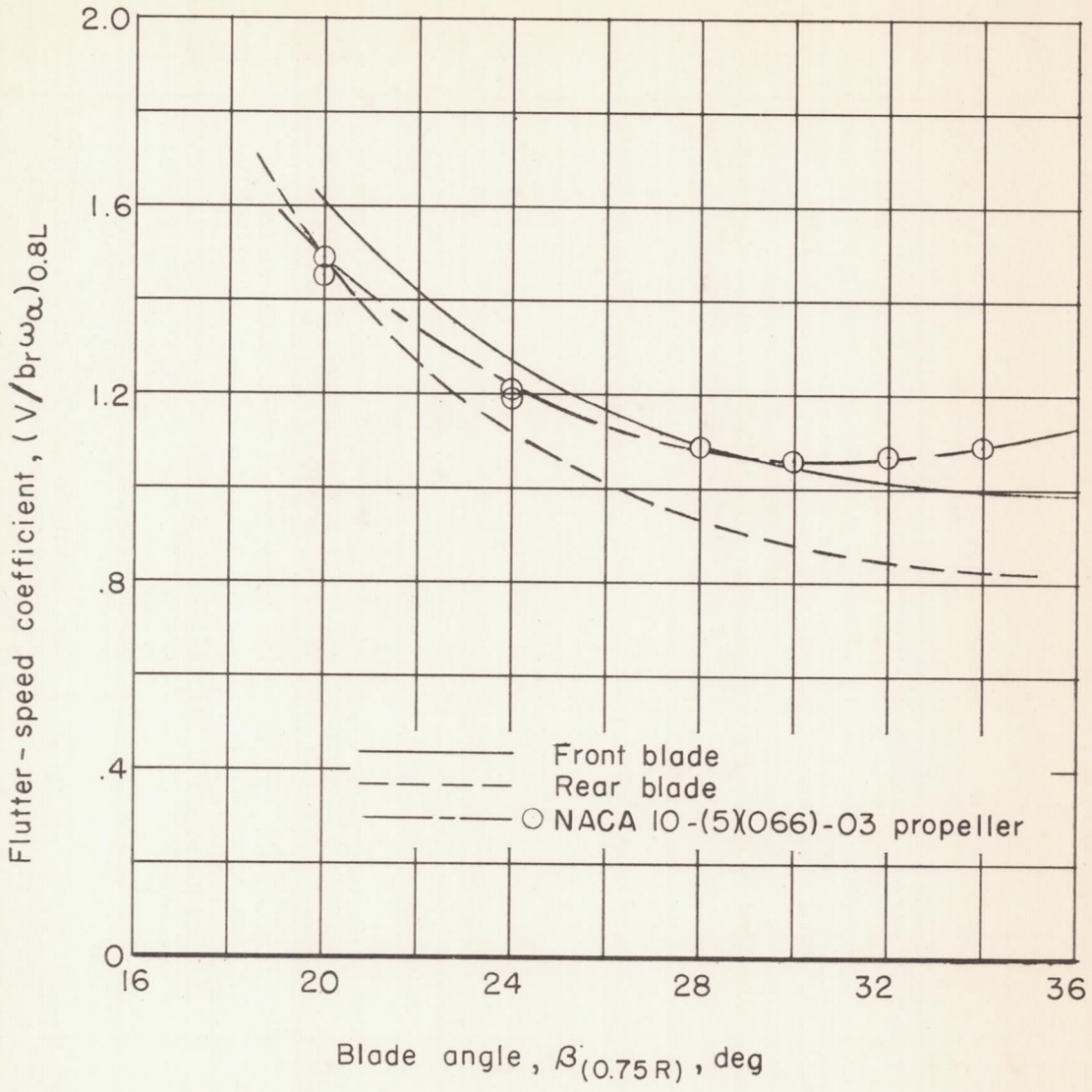

Figure 11.- Comparison of the stall-flutter boundaries of front and rear propeller blades of six- and eight-blade configurations. Torsional stress = ±2,000 lb/in.^{2}; flutter characteristics of NACA 10-(5)(066)-03 single-rotating propeller of reference 7.

NACA-Langley - 2-4-55 - 350